

Linear cosmological Perturbations in scalar-tensor-vector gravity

Sara Jamali^a, Mahmood Roshan^{a,b,*} and Luca Amendola^c

^aDepartment of Physics, Faculty of Science, Ferdowsi University of Mashhad P.O. Box 1436, Mashhad, Iran

^bSchool of Astronomy, Institute for Research in Fundamental Sciences (IPM), P.O. Box 19395-5531, Tehran, Iran

^cInstitute for Theoretical Physics, University of Heidelberg, Philosophenweg 16, D-69120 Heidelberg, Germany

ARTICLE INFO

Keywords:

Modified gravity
Structure formation
Linear perturbations
Dark matter
Scalar-tensor-vector gravity

ABSTRACT

We investigate the cosmological perturbations in the context of a Scalar-Tensor-Vector theory of Gravity known as MOG in the literature. Recent investigations show that MOG reproduces a viable background cosmological evolution comparable to Λ CDM. However, the matter dominated era is slightly different. In this paper, we study the linear matter perturbations and estimate the relevant modified gravity parameters. We show that MOG reduces the growth rate of the perturbations and comparing with the RSD data reveals that MOG suggests a higher value for σ_8 , compare to Λ CDM. This point, constitute a powerful challenge to the cosmological viability of MOG.

1. Introduction

The Scalar-Vector-Tensor theory of gravity, also known as MOG in the literature, has been introduced in [1]. MOG does not includes dark matter but introduces instead two scalar fields, G and μ , and one vector field, ϕ_α , in addition to the metric tensor. Although MOG is plagued by ghosts, it does not suffer from the tachyonic instability, which means that in the non-quantum limit, that is suitable for the cosmological implications, MOG can be considered as a viable theory [2]. We assume the quantum ghost instability can be cured by additional terms relevant at high energies but unimportant at the classical low-energy level investigated in this paper. Although developing a ghost free version of MOG would be interesting, in order to compare our results with those already claimed in the literature, we use the original version of MOG investigated almost in all the previous works.

The astrophysical consequences of MOG have been widely investigated in, for example, [3]-[4]. In [3], it has been shown that MOG can explain the flat rotation curve of spiral galaxies without invoking dark matter particles. It is shown in [5] that MOG can also explain the mass discrepancy in galaxy clusters. In the strong field limit, MOG black holes have been also investigated in the literature, for example see [6]-[7]. While MOG is consistent with the recently discovered gravitational wave signals [8], it has been shown in [9] that the quasinormal modes of gravitational perturbations in the ringdown phase of the merging of two MOG black holes have different frequencies compared to those of GR. In [10], using dynamical system approach, It is shown that The cosmic evolution starts from a standard radiation dominated era, evolves towards a matter dominated epoch and tends to a late time accelerated phase. In [2], we showed that MOG cannot fit the observational data of the sound horizon angular size. However, a slightly modified version of MOG, called mMOG, gives a good agreement with the sound horizon data, although the matter dominated era of mMOG re-

mains slightly different from Λ CDM.

It is claimed in the literature, [11, 12], that MOG increases the growth rate of matter perturbations, compared to Λ CDM. Although they use the modified Poisson equation in MOG obtained in a non-expanding universe and also ignore the evolution of perturbations in the scalar field G . In this paper we revisit the linear perturbations in MOG and compare it with Λ CDM, without any of these restrictive assumptions. We find a slower growth and comparing MOG to the available redshift space distortion (RSD) data, a higher value for σ_8 . Although *per se* this fact does not rule out MOG, such a high value will probably be in conflict with lensing and CMB results.

2. The Scalar-Tensor-Vector theory

The action of Scalar-Tensor-Vector theory of Gravity, known also as MOG [13], is

$$S = S_{\text{gravity}} + S_{\text{scalar fields}} + S_{\text{vector field}} + S_{\text{m}} \quad (1)$$

in which,

$$S_{\text{gravity}} = \int \sqrt{-g} d^4x \left(\frac{R - 2\Lambda}{16\pi G} \right) \quad (2)$$

$$S_{\text{scalar fields}} = \int \sqrt{-g} d^4x \frac{1}{2G} g^{\mu\nu} \left(\frac{\nabla_\mu G \nabla_\nu G}{G^2} + \frac{\nabla_\mu \mu \nabla_\nu \mu}{\mu^2} \right) \quad (3)$$

$$S_{\text{vector field}} = \int \sqrt{-g} d^4x \frac{1}{4\pi} \left(\frac{1}{4} B_{\mu\nu} B^{\mu\nu} + V_\phi \right) \quad (4)$$

where R is the Ricci scalar, Λ is the effective cosmological constant and the anti-symmetric tensor $B_{\mu\nu}$ is written as $\nabla_\mu \phi_\nu - \nabla_\nu \phi_\mu$, where ϕ_μ is the vector field.

The vector field potential V_ϕ is set to $-\frac{1}{2}\mu^2\phi_\alpha\phi^\alpha$, in which μ , in general, is a scalar field which plays the role of the mass of the vector field. This potential is the original form introduced in [1], that also leads to a viable weak field limit and also to an acceptable sequence of cosmic epochs. The action of matter, $S_{\text{m}}(g_{\alpha\beta}, \phi_\alpha)$, is postulated to be coupled to

*Corresponding author

✉ sara.jamali@um.ac.ir (S. Jamali); mroshan@um.ac.ir (M. Roshan);

l.amendola@thphys.uni-heidelberg.de (L. Amendola)

ORCID(S):

the vector field. In this case, there will be a non-zero fifth force current J_α . For the sake of simplicity and without loss of generality, we set the scalar field μ constant during the structure formation era. It should be mentioned that this scalar field does not play a crucial role in the cosmic history of MOG [14] and [15]. More specifically it is shown in [2] and [10] that μ does not carry a substantial contribution to the total energy budget. In contrast, the scalar field G seriously influences the dynamics of the gravitating systems [5, 3].

The energy-momentum tensors associated with the scalar field \mathcal{G} , defined as $\mathcal{G} = 1/G$, and with the vector field ϕ_α , are defined as $-\frac{2}{\sqrt{-g}} \frac{\delta S_{\text{field}}}{\delta g^{\mu\nu}}$, and results in

$$T_{\mu\nu(\mathcal{G})} = -\frac{\nabla_\mu \mathcal{G} \nabla_\nu \mathcal{G}}{\mathcal{G}} + \frac{1}{2} g_{\mu\nu} \frac{\nabla_\alpha \mathcal{G} \nabla^\alpha \mathcal{G}}{2\mathcal{G}}, \quad (5)$$

$$T_{\mu\nu(\phi_\alpha)} = -\frac{1}{4\pi} \left[B_\mu^\alpha B_{\nu\alpha} - g_{\mu\nu} \left(\frac{1}{4} B^{\rho\sigma} B_{\rho\sigma} + V_\phi \right) + 2 \frac{\partial V_\phi}{\partial g^{\mu\nu}} \right]. \quad (6)$$

Now let us briefly review the field equations of the theory. Variation of the action (1) with respect to $g^{\mu\nu}$, yields the following modified Einstein equation

$$G_{\mu\nu} - \frac{\nabla_\mu \nabla_\nu \mathcal{G}}{\mathcal{G}} + g_{\mu\nu} \frac{\square \mathcal{G}}{\mathcal{G}} + \Lambda \mathcal{G} g_{\mu\nu} = \frac{8\pi}{\mathcal{G}} (T_{\mu\nu(\mathcal{G})} + T_{\mu\nu(\phi_\alpha)} + T_{\mu\nu(m)}) \quad (7)$$

where $T_{\mu\nu(m)} = -\frac{2}{\sqrt{-g}} \frac{\delta S_m}{\delta g^{\mu\nu}}$ and $G_{\mu\nu}$ is the Einstein tensor. On the other hand, by varying the actions (3) and (4) with respect to \mathcal{G} and ϕ_α , the following field equations can be derived

$$\square \mathcal{G} = \frac{1}{16\pi} R \mathcal{G} + \frac{1}{2\mathcal{G}} \nabla_\alpha \mathcal{G} \nabla^\alpha \mathcal{G} - \frac{\Lambda \mathcal{G}}{8\pi} \quad (8)$$

$$\nabla_\beta B^{\beta\alpha} = 4\pi J^\alpha - \mu^2 \phi^\alpha \quad (9)$$

where the d'Alembertian operator $\square \mathcal{G}$ is defined as $\nabla_\alpha \nabla^\alpha \mathcal{G}$, and the fifth force current is obtained by varying the matter action with respect to the vector field as $J^\alpha = \frac{1}{\sqrt{-g}} \frac{\delta S_m}{\delta \phi_\alpha}$. Now, using (8), we can find the following continuity equations for \mathcal{G} and ϕ_α

$$\nabla_\mu T_{\nu(\phi_\alpha)}^\mu = B_{\alpha\nu} J^\alpha - \frac{1}{4\pi} \frac{\partial V_\phi}{\partial \phi_\alpha} B_{\nu\alpha} + \frac{\nabla_\nu V_\phi}{4\pi} - \frac{1}{2\pi} \nabla^\mu \left(\frac{\partial V_\phi}{\partial g^{\mu\nu}} \right) \quad (10)$$

$$\nabla_\mu T_{\nu(\mathcal{G})}^\mu = -\frac{R}{16\pi} \nabla_\nu \mathcal{G} + \frac{\Lambda}{8\pi} \nabla_\nu \mathcal{G}. \quad (11)$$

We suppose that the matter content of the universe is a perfect fluid. In this case, by assuming the continuity relation $\nabla_\alpha J^\alpha = 0$ (or equivalently $\nabla_\alpha \phi^\alpha = 0$), one finds

$$\nabla_\alpha T_{\nu(m)}^\alpha = -B_{\alpha\nu} J^\alpha, \quad (12)$$

(see [16] for more details). The assumption of isotropy and homogeneity leads to $B_{\alpha\nu} = 0$ at the background level. Therefore, by using eq. (12), one recovers the normal continuity equation for the ordinary matter.

It is convenient now to rewrite the relevant background equations using the e -folding time $\tau = \ln a$ and $\mathcal{H} = Ha$, the conformal Hubble function:

$$\frac{\mathcal{G}'}{\mathcal{G}} = -\frac{\mathcal{G}' \mathcal{H}'}{\mathcal{G} \mathcal{H}} + \frac{\mathcal{G}''}{2\mathcal{G}^2} - \frac{2\mathcal{G}'}{\mathcal{G}} - \frac{3\mathcal{H}'}{8\pi \mathcal{H}} - \frac{3}{8\pi} + \frac{e^{2\tau} \Lambda}{8\pi \mathcal{H}^2}, \quad (13)$$

$$J_{0\tau}(\tau) = \frac{\mu^2 \phi_{0\tau}}{4\pi} \quad (14)$$

where a prime stands for derivative with respect to τ . As we shall see, equations (13) and (14) are necessary to simplify the first order equations. In the following section, we linearize these equations and investigate the growth of density perturbations.

3. The perturbed equations

Let us start with the following perturbed flat-space metric in the Newtonian gauge

$$ds^2 = e^{2\tau} \left[-(1 + 2\Psi) \mathcal{H}^{-2} d\tau^2 + (1 + 2\Phi) \delta_{ij} dx^i dx^j \right] \quad (15)$$

We work from now on in Fourier space, with \mathbf{k} denoting the wavevector. One can write the perturbed fields ϕ_α and \mathcal{G} as

$$\begin{aligned} \phi_\alpha &= (\phi_\tau, \phi_i) = (\phi_{0\tau}(\tau) + \phi_{1\tau}(\tau) e^{i\mathbf{k}\cdot\mathbf{r}}, ik\phi_{1i}(\tau) e^{i\mathbf{k}\cdot\mathbf{r}}) \\ \mathcal{G}(\tau) &= \mathcal{G}_0(\tau) + \mathcal{G}_1(\tau) e^{i\mathbf{k}\cdot\mathbf{r}} \end{aligned} \quad (16)$$

where the subscript \mathbf{i} stands for any of three spatial components, i.e. (x, y, z) , and both background and perturbed quantities are functions of τ . From now on, the subscripts 0 and 1 specify the background and the first order perturbed fields, respectively.

We perturb now the energy-momentum tensors. Let us start with the energy-momentum tensor of the ordinary matter. In this case it is straightforward to show that

$$\begin{aligned} T_{0(m)}^0 &= -(\rho + \delta\rho) e^{i\mathbf{k}\cdot\mathbf{r}} \\ T_{0(m)}^i &= \frac{i}{\sqrt{3}k} \rho \theta (\omega + 1) e^{i\mathbf{k}\cdot\mathbf{r}} \\ T_{\mathbf{i}(m)}^j &= (\rho \omega + c_s^2 \delta\rho) e^{i\mathbf{k}\cdot\mathbf{r}} + \Sigma_{\mathbf{i}}^j \end{aligned} \quad (17)$$

where ω is the equation of state parameter, $\delta = \frac{\delta\rho}{\rho}$ is the density contrast, ρ is the background density, $\theta = i\mathbf{k}\cdot\mathbf{v}/\mathcal{H}$ is the velocity divergence and \mathbf{v} is the peculiar velocity. Perturbations in the fluid pressure p is given by $\delta p = c_s^2 \delta\rho$, where c_s^2 is the adiabatic sound speed of the fluid. Since matter is supposed to be approximated by a perfect fluid, we ignore the anisotropic stress tensor $\Sigma_{\mathbf{i}}^j$.

Similarly, in the following we linearize the energy-momentum tensors associated with the fields \mathcal{G} and ϕ_α . To do so, we use equation (5), and find the first order perturbation of $T_{(\mathcal{G})}^{\mu\nu}$ shown as $\delta T_{(\mathcal{G})}^{\mu\nu}$. The result is

$$\begin{aligned} \delta T_{0(\mathcal{G})}^0 &= \frac{\mathcal{H}^2 \mathcal{G}'_0}{2\mathcal{G}_0^2} \left(2\mathcal{G}_0 (\mathcal{G}'_1 - \Psi \mathcal{G}'_0) - \mathcal{G}_1 \mathcal{G}'_0 \right) e^{-2\tau + i\mathbf{k}\cdot\mathbf{r}}, \\ \delta T_{0(\mathcal{G})}^i &= -\frac{ik\mathcal{G}_1 \mathcal{G}'_0}{\sqrt{3}\mathcal{G}_0} e^{-2\tau + i\mathbf{k}\cdot\mathbf{r}} \end{aligned} \quad (18)$$

and $\delta T_{0(\mathcal{G})}^0 = -\delta T_{\mathbf{i}(\mathcal{G})}^{\mathbf{i}}$. In a similar way, for the vector field ϕ_α , using equation (6), we have

$$\delta T_{0(\phi_\alpha)}^0 = -\delta T_{\mathbf{i}(\phi_\alpha)}^{\mathbf{i}} = \frac{\mu^2 \mathcal{H}^2 \phi_{0\tau}}{4\pi} \left(\phi_{1\tau} - \phi_{0\tau} \Psi \right) e^{-2\tau + i\mathbf{k}\cdot\mathbf{r}},$$

$$\delta T_{0(\phi_\alpha)}^i = \frac{ik}{4\pi} \mu^2 \phi_{1i} \phi_{0\tau} e^{-2\tau+ik\cdot\mathbf{r}} \quad (19)$$

Now, to find the linearized form of the conservation equations (10) and (11), we first start with the scalar field \mathcal{G} and use equations (11) and (5) to find the first order relations. In this case the covariant derivative of (5) and the right hand side of equation (11) at the perturbed level can be straightforwardly calculated. Since they are long to be written here, we refer the reader to this explanation, if it is needed. In fact, the spatial component gives rise to a trivial relation. Notice that to show this, one needs to insert the background equation for \mathcal{G}'_0 given in (13). On the other hand, the time component leads to a second-order differential equation for \mathcal{G}_1 , see equation (34). We will discuss this relation in the next section.

Now we return to the vector field's conservation equation (10). Let us first use equation (19) and linearize the left hand side of equation (10). The result is

$$\begin{aligned} \nabla_\mu \delta T_i^\mu(\phi_\alpha) &= -\frac{ik\mu^2 \mathcal{H}^2}{12\pi} \phi_{0\tau} \left(\sqrt{3}\phi_{1\tau} - 3\phi'_{1i} \right) e^{-2\tau+ik\cdot\mathbf{r}} \\ \nabla_\mu \delta T_0^\mu(\phi_\alpha) &= 0 \end{aligned} \quad (20)$$

By keeping the first order terms on the right-hand side of (10), one can easily show that the time component vanishes. For the spatial components, it turns out that only the first term on the right-hand side contributes. Therefore the spatial component on the right hand side of (10) in the linear limit is written as

$$(B_{ai}J^\alpha)_1 = -\frac{1}{3} ik \mathcal{H}^2 J_{0\tau} \left(\sqrt{3}\phi_{1\tau} - 3\phi'_{1i} \right) e^{-2\tau+ikr} \quad (21)$$

Equating now eqs. (20) and (21), and summing over the index i , one may easily find the following scalar equation

$$ik\mathcal{H}^2 e^{-2\tau+ik\cdot\mathbf{r}} \left(4\pi J_{0\tau} - \mu^2 \phi_{0\tau} \right) \left(\sqrt{3}\phi_{1\tau} - A'_1 \right) = 0 \quad (22)$$

where A_1 is $\sum_i \phi_{1i}$, and accordingly $A'_1 = \sum_i \phi'_{1i}$. However, by using the vector field equation (9), one can readily conclude that the first parenthesis of (22) vanishes, see equation (14). Moreover, by using the field equation of ϕ_α , we show now that the second parentheses is also zero. Let us first take the divergence of (9) by keeping in mind that $\nabla_\alpha \phi^\alpha = 0$ and $\nabla_\alpha J^\alpha = 0$. Consequently we arrive at a constraint identity on $B_{\alpha\beta}$, namely $\nabla_\alpha \nabla_\beta B^{\alpha\beta} = 0$. By linearizing this constraint we find

$$(\mathcal{H}^5 - \mathcal{H})(f') + \mathcal{F}(\mathcal{H})f = 0 \quad (23)$$

where the function f is defined as $f = \sqrt{3}\phi_{1\tau} - A'_1$ and \mathcal{F} is $(6e^{2\tau}\mathcal{H}^3 - 4\mathcal{H}^4\mathcal{H}' - e^{2\tau}\mathcal{H}^2\mathcal{H}' - \mathcal{H}' + 4\mathcal{H}^5)$. One may straightforwardly conclude that $f = 0$. On the other hand, spatial isotropy implies that $A = \phi_{1x} + \phi_{1y} + \phi_{1z} = 3\phi_{1j}$, where $j = 1, 2, 3$. This directly yields a simple differential equation between vector field components as

$$\phi'_{1j} = \frac{\phi_{1\tau}}{\sqrt{3}} \quad (24)$$

which is equivalent to $A'_1 = \sqrt{3}\phi_{1\tau}$ and consequently we have $\nabla_\mu \delta T_{\nu(\phi_\alpha)}^\mu = 0$, or equivalently $(B_{\alpha\nu}J^\alpha)_1 = 0$. This result has an interesting consequence. In fact, it shows that $T_{(m)}^{\mu\nu}$ is conserved even in the linearized limit, i.e. $\nabla_\mu \delta T_{\nu(m)}^\mu = 0$, see equation (12). This conservation equation along with the relation (17) leads to the following expressions

$$\begin{aligned} \delta k^2 c_s^2 + \theta \mathcal{H} \left((\omega + 1) (\mathcal{H}(3\omega - 1) - \mathcal{H}') - \mathcal{H}\omega' \right) \\ + \mathcal{H}^2(\omega + 1)\theta' - k^2\Psi(\omega + 1) = 0 \end{aligned} \quad (25)$$

$$3\delta c_s^2 + \delta' + \theta + 3\Phi' - 3\delta\omega + \theta\omega + 3\omega\Phi' = 0 \quad (26)$$

where (25) is obtained from the spatial component $\nabla_\mu \delta T_{i(m)}^\mu = 0$, and (26) is the corresponding time component.

Let us now summarize this section by considering the number of unknowns and equations. There are seven unknown perturbation quantities: G_1 , $\phi_{1\tau}$, ϕ_{1i} , ρ , θ , Ψ and Φ . Accordingly, we need seven equations to describe the evolution of the perturbed quantities. Three equations are given by the conservation equations. More specifically, the conservation equation of $T_{(\mathcal{G})}^{\mu\nu}$, i.e. equation (11) yields a differential equation for \mathcal{G}_1 , see equation (34) in the next section, while the conservation equation for $T_{(m)}^{\mu\nu}$ gives the two differential equations (25) and (26). Moreover, using the identity $\nabla_\alpha \nabla_\beta B^{\alpha\beta} = 0$, we found a relation between the components of the vector field, see equation (24). Consequently, we still need three equations to construct a complete set of equations. To find these three equations, in the next section we use the time component of the vector field equation (9), along with the off-diagonal and time components of the field equation (7).

4. Perturbations in the sub-horizon scale

In this section, we investigate the evolution of the density parameter δ in the sub-horizon scale. Specifically, the sub-horizon scale corresponds to the scale at which the physical wavelength $2\pi a/k$ is much smaller than the Hubble radius $1/H$. In order to apply the sub-horizon limit to the perturbed equations, we introduce the dimensionless length parameter $\lambda = \mathcal{H}/k$ and perform the limit $\lambda \ll 1$, keeping only terms up to the lowest order. We restrict ourselves to the matter dominated epoch in MOG, where structure formation occurs. Therefore it is natural to expect that the equation of state parameter and the sound speed are zero, i.e. $\omega = 0$ and $c_s^2 = 0$.

Keeping these assumptions in mind, the off-diagonal component of (7), leads to the following relation

$$\Phi + \Psi = -\frac{\mathcal{G}_1}{\mathcal{G}_0} \quad (27)$$

Now, equation (26) can be written as

$$\delta' + 3(c_s^2 - \omega)\delta = -(\theta + 3\Phi')(\omega + 1) \quad (28)$$

On the other hand equation (25) gives

$$\theta' - \left(\frac{6\omega + 3\omega_t - 1}{2} - \frac{\omega'}{1 + \omega} \right) \theta = \frac{1}{\lambda^2} \left(\frac{c_s^2 \delta}{1 + \omega} + \Psi \right) \quad (29)$$

where we have conveniently defined the total equation of state parameter ω_t as follows

$$\frac{H'}{H} = 1 + \frac{H'}{H} = -\frac{1}{2} - \frac{3}{2} \omega_t. \quad (30)$$

Differentiating (28) with respect to $\tau = \ln a$, and combining with (29), we arrive at

$$\delta'' = \frac{1}{2}(3\omega_t - 1)(\delta' + 3\Phi') + \frac{1}{\lambda^2} \left(\frac{\mathcal{G}_1}{\mathcal{G}_0} + \Phi \right) - 3\Phi''. \quad (31)$$

As we already mentioned, in the sub-horizon limit, we ignore Φ'' and Φ' in comparison with $\frac{\Phi}{\lambda^2}$. In order to find a relation between Φ and \mathcal{G}_1 , we exploit the perturbed time component of equation (7) and also we apply the sub-horizon limit for \mathcal{G} to find

$$\frac{\Phi}{\lambda^2} + \frac{1}{\mathcal{G}_0} \left(\frac{\mathcal{G}_1}{2\lambda^2} - \frac{4\pi\rho\delta}{e^{-2\tau}\mathcal{H}^2} - \mu^2\phi_{0\tau}\phi_{1\tau} \right) = 0 \quad (32)$$

Now we need to find the last term, i.e., $\mu^2\phi_{0\tau}\phi_{1\tau}$, in terms of the other perturbations. In order to quantify this term, we perturb the vector field equation (9). The vector field J^α is defined [15] as $\kappa\rho_m u^\alpha$, where u^α is the four-velocity, and ρ_m is the matter density. Using equation (9) the vector field J_α is also specified. One can straightforwardly check that the constraints on ϕ_α and J_α , i.e. $\nabla_\alpha\phi^\alpha = 0$ and $\nabla_\alpha J^\alpha = 0$, do not add new first order equations for the vector fields.

Now, let us return to equation (32) in which one can replace $\mu^2\phi_{0\tau}\phi_{1\tau}$ using equations (9) and the definition of J^α , as explained above. We ignore the term including Ψ in comparison with $\frac{\Phi}{\lambda^2}$. Finally equation (32) takes the following form

$$\frac{\Phi}{\lambda^2} + \frac{1}{\mathcal{G}_0} \left(\frac{\mathcal{G}_1}{2\lambda^2} - \frac{4\pi\rho\delta}{e^{-2\tau}\mathcal{H}^2} - \left(\frac{4\pi\kappa\rho}{e^{-\tau}\mathcal{H}\mu} \right)^2 \delta \right) = 0 \quad (33)$$

In order to find the perturbed fields \mathcal{G}_1 , Φ and Ψ , we use the time component of the conservation equation of $T_G^{\mu\nu}$. In fact, we use this relation instead of the field equation of \mathcal{G} given by (8). Keeping the lowest order of λ , the result takes the following simple form

$$\frac{\mathcal{G}_1}{\lambda^2} + \frac{\mathcal{G}_0}{8\pi\lambda^2}(\Psi + 2\Phi) = 0 \quad (34)$$

Now, we have equations (27), (33) and (34) for three unknowns \mathcal{G}_1 , Φ and Ψ . Some algebraic manipulations gives

$$\begin{aligned} \Psi &= -\frac{16\pi(4\pi-1)\lambda^2\rho(4\pi\kappa^2\rho+\mu^2)}{(16\pi-3)\mathcal{G}\mathcal{H}^2e^{-2\tau}\mu^2}\delta \\ \Phi &= \frac{8\pi(8\pi-1)\lambda^2\rho(4\pi\kappa^2\rho+\mu^2)}{(16\pi-3)\mathcal{G}\mathcal{H}^2e^{-2\tau}\mu^2}\delta \\ \mathcal{G}_1 &= -\frac{8\pi\lambda^2\rho(4\pi\kappa^2\rho+\mu^2)}{(16\pi-3)e^{-2\tau}\mathcal{H}^2\mu^2}\delta \end{aligned} \quad (35)$$

As an aside, one can immediately derive the anisotropic stress $\eta = -\Phi/\Psi$ as follows

$$\eta = \frac{8\pi-1}{8\pi-2} \approx 1.04 \quad (36)$$

This quantity, which is unity in the standard case, can be measured by combining weak lensing and galaxy clustering. Although present constraints on this parameter are still very weak, in [17] it has been shown that a Euclid-like survey can measure a constant η to within a few percent. This might then be an additional way to distinguish MOG from standard gravity.

From now on, we focus on the matter perturbation growth. In the context of MOG, the evolution of density contrast in the matter dominated era takes the form

$$\delta'' + \left(\frac{1}{2} - \frac{3\omega_t}{2} \right) \delta' - \frac{4\pi-1}{16\pi-3} \left(\frac{16\pi(4\pi\kappa^2\rho+\mu^2)}{\mathcal{G}_0\mathcal{H}^2\mu^2e^{-2\tau}} \right) \delta\rho = 0. \quad (37)$$

To simplify this equation, we first replace \mathcal{G}_0 by $1/G_0$, then ρ by $\frac{3\mathcal{H}^2e^{-2\tau}\Omega_m}{8\pi G_0}$ and the term $\mathcal{H}e^{-\tau}$ by H . Finally, we find

$$\delta'' + \left(\frac{1}{2} - \frac{3\omega_t}{2} \right) \delta' - \frac{(4\pi-1)}{(16\pi-3)} \left(\frac{6H^2\kappa^2\Omega_m}{G_0\mu^2} + 4 \right) \frac{3}{2}\Omega_m\delta = 0. \quad (38)$$

The coefficient

$$Y \equiv \frac{(4\pi-1)}{(16\pi-3)} \left(\frac{6H^2\kappa^2\Omega_m}{G_0\mu^2} + 4 \right) \quad (39)$$

represents the modification of the Poisson equation induced by MOG terms. One has $Y = 1$ in the standard gravity. This coefficient is variously denoted as G_{eff} or μ in current literature. Together with η given above, it fully characterizes the theory at linear, quasi-static scales.

In order to simplify equation (38), we use some results from [2] to write the following relation. Moreover, one can check that Ω_μ is almost negligible during the cosmic evolution, which confirms our assumption that μ is almost constant.

$$\frac{12H^2\kappa^2\Omega_m^2}{G_0\mu^2} = 1 - (\Omega_m + \Omega_R + \Omega_G + \Omega_\Lambda) \quad (40)$$

and combining equations (38) and (40), we arrive at

$$\delta'' + \left(\frac{1}{2} - \frac{3\omega_t}{2} \right) \delta' - \frac{3}{2}\Omega_m Y_{\text{MOG}}\delta = 0. \quad (41)$$

where now we see that

$$Y_{\text{MOG}} = \frac{(4\pi-1)}{2\Omega_m(16\pi-3)} \left(1 - \Omega_R - \Omega_G - \Omega_\Lambda + 7\Omega_m \right) \quad (42)$$

This is the main expression needed to investigate the linear perturbations in MOG. Let us compare it with the corresponding equation in Λ CDM, namely

$$\delta'' + \left(\frac{1}{2} - \frac{3\omega_t}{2} \right) \delta' - \frac{3}{2}\Omega_m\delta = 0. \quad (43)$$

It is clear that the main difference between equations (41) and (43) is the coefficient Y , since ω_t evolves similarly in

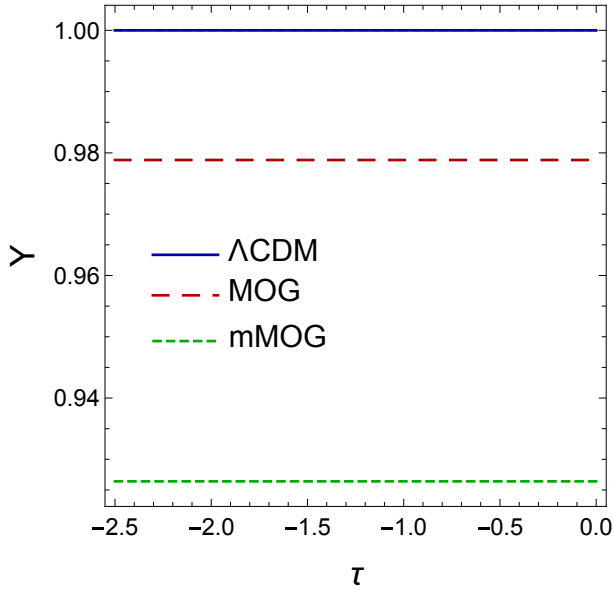


Figure 1: The evolution of the coefficients Y_{MOG} and Y_{mMOG} for $c = 0.33 \times 8\pi$ is compared to the ΛCDM case, i.e., the blue line $Y = 1$. The smaller Y for MOG and mMOG results in a slower growth rate.

both MOG and ΛCDM [2]. This coefficient can qualitatively specify whether the growth rate in MOG is lower or higher than that of ΛCDM . Using the numerical solutions, the evolution of Y is shown in Fig. 1, for MOG, mMOG and ΛCDM . The magnitude of Y in MOG and mMOG is smaller than ΛCDM . Therefore one may expect a slower growth rate for matter perturbations in MOG.

5. Numerical integration

Now, let us solve (41) by choosing a suitable set of initial conditions. We begin with the simplest choice, that is, the same initial conditions of ΛCDM in the deep matter dominated phase, namely

$$\delta'(\tau^*) = \delta(\tau^*), \quad \delta(\tau^*) = a^*. \quad (44)$$

where the initial $\tau^* = \ln a^*$ is taken at $\tau = -2.5$, which corresponds to the redshift $z^* \simeq 11$. As advertised, and as we found, solving (41), δ in MOG grows slower than in ΛCDM .

The initial conditions in modified theories of gravity, in principle, can be different from ΛCDM , for example see [18]. Consequently, we generalize the initial conditions as

$$\delta'(\tau^*) = \beta \delta(\tau^*) \quad (45)$$

where the new parameter, β , expresses the deviation from ΛCDM initial conditions. We need to consider only $\beta < 1$ since we checked analytically that in matter dominated era of MOG, we have always $\delta'/\delta < 1$. We also checked that for any β the evolution of δ reverts soon back to the case $\beta = 1$. The conclusion that the growth of δ in MOG is slower than ΛCDM does not depend therefore on the initial conditions.

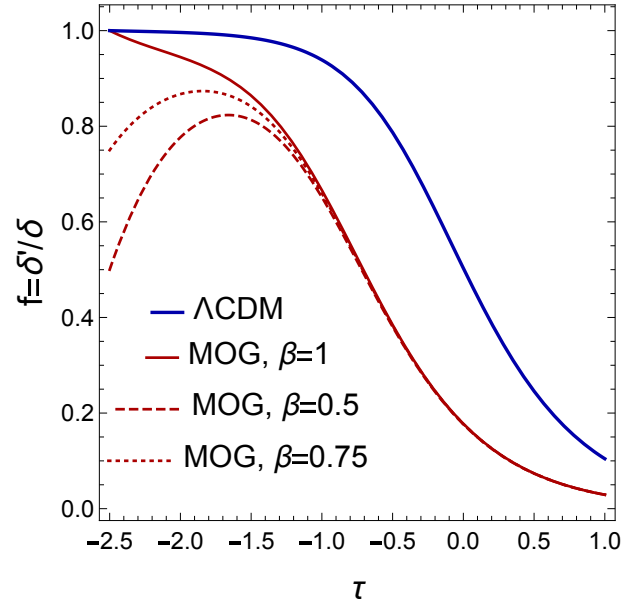


Figure 2: The growth rate function in MOG and ΛCDM . The initial conditions are $f(-2.5) = 1$ for ΛCDM and $f(-2.5) = \beta$ for MOG.

It is also instructive to investigate the growth rate f of matter perturbations, defined as follows

$$f = \frac{\delta'}{\delta} = \frac{d \ln \delta}{d \ln a} \quad (46)$$

Equation (41) can be written in terms of f as

$$f' + f^2 + \frac{1}{2}(1 - 3\omega_t)f - \frac{3}{2}\Omega_m Y_{\text{MOG}} = 0. \quad (47)$$

To solve this equation, we need only one initial condition, (45), namely $f(z^*) = \beta$. The result is illustrated in Fig. 2, that clearly confirms the growth parameter f in MOG is always smaller than the standard case, regardless of β . We now proceed to evaluate the growth rate in mMOG, a modified version of MOG in which a new free parameter c has been incorporated by changing the kinetic energy contribution of the scalar field G and it turns out that for the value $c = 0.33 \times 8\pi$, it brings the sound horizon angular size compatible with the observation, while at the same time achieving a viable sequence of cosmological epochs [2]. Following the same steps as for MOG, we find

$$\delta'' + \left(\frac{1}{2} - \frac{3\omega_t}{2} \right) \delta' - \frac{3}{2} Y_{\text{mMOG}} \Omega_m \delta = 0. \quad (48)$$

where

$$Y_{\text{mMOG}} = \frac{(c-2)}{(8c-12)\Omega_m} \left(1 - \Omega_R - \Omega_G - \Omega_\Lambda + 7\Omega_m \right) \quad (49)$$

where $\Omega_G = \frac{G'}{G} - \frac{c}{6} \left(\frac{G'}{G} \right)^2$ and the other Ω 's are the same as in MOG. In order to avoid the existence of tachyonic instability, we restrict ourselves to positive c . We find the exact numeric solution of (48) for the same initial conditions described for MOG. Our solution shows that the new parameter c does not lead to a significant deviation from MOG. The

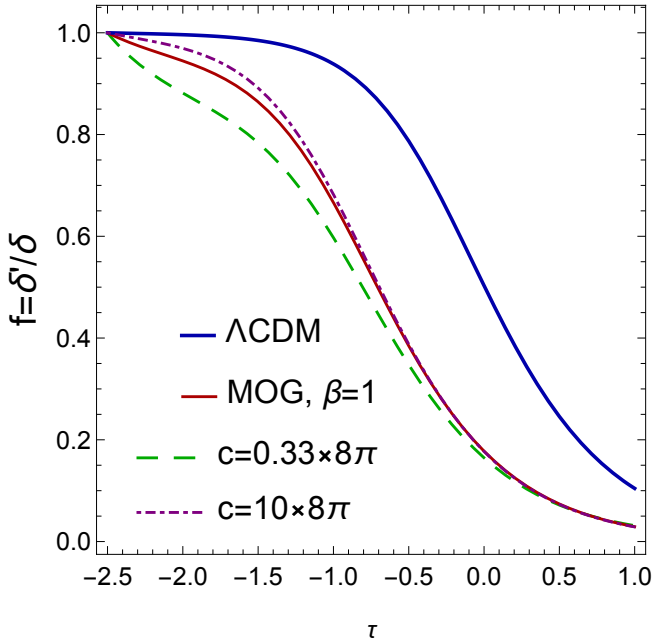


Figure 3: The behavior of f in mMOG for different choices of c and Λ CDM. The growth of perturbations in mMOG is slower than Λ CDM, using the same initial condition, $f(-2.5) = 1$

corresponding growth rate parameter f , for different values of c , is plotted in Fig. 3.

We can simply conclude that both MOG and mMOG lead to slower matter growth compared to Λ CDM. The reason is that the rate of growth depends heavily on the fraction of matter compared to other energy contributions. If the other homogeneous fields decrease this fraction, as it occurs here, the effect overcompensates the increase of gravitational strength, and the result is less growth.

In the following section, we compare our results with the relevant observation and discuss the viability of MOG as an alternative to dark matter particles.

6. Comparison with observation

In the previous section, we have obtained the evolution of the growth function f in the context of MOG and a slightly modified version called mMOG. Here, we use the available data for $f\sigma_8$ to compare (48) with observation. The RSD parameter, $f\sigma_8$, is defined as

$$f\sigma_8 \equiv \sigma_8(z) \frac{\delta'(z)}{\delta(z)}; \quad \text{where} \quad \sigma_8(z) = \sigma_8^0 \frac{\delta(z)}{\delta(0)}. \quad (50)$$

To obtain the current value of σ_8 , it is necessary to specify the underlying gravity theory. Then σ_8^0 is determined through model dependent observations such as CMB power spectrum [19], weak lensing [20] and abundance of clusters [21]. Consequently, σ_8^0 is a model-dependent quantity [22], and naturally one may expect a different value for it in MOG compared with Λ CDM (where $\sigma_8^0 = 0.802 \pm 0.018$ [19]), as we are going to find now.

We assume that $f\sigma_8(z)$ data are also valid in MOG¹. Then we solve the perturbation equation (48), and by fitting to $f\sigma_8(z)$ data, we predict the best value for σ_8^0 in MOG. It is worth mentioning that the available data for $f\sigma_8$ lie in the redshift range $0 \leq z \leq 1.2$ (see Fig. 4). In this interval, the baryonic matter, the cosmological constant and the scalar field G have non-zero contribution to the energy budget of the Universe, see Fig. 1 in [2]. On the other hand, one can ignore radiation in equation (48).

As we already discussed, equation (41) needs two initial conditions to be solved. Consequently, we have two free parameters σ_8^0 and β . However, we have already discussed in the previous section that the evolution of perturbations does not change significantly with initial conditions, essentially because the growing mode dominates, regardless of the initial conditions. Therefore, without loss of generality, we set $\beta = 1$ as in Λ CDM.

For the data points, D_i , we used Table II in [23]. In the case of independent data points, the likelihood function \mathcal{L} is given by a simple relation,

$$\mathcal{L} = A \exp[-\chi^2/2] \quad (51)$$

in which A is a normalization constant and χ^2 is defined as

$$\chi^2 = \sum_i \frac{(D_i - \mathcal{T}_i)^2}{\sigma_i^2} \quad (52)$$

where D_i and \mathcal{T}_i refer to the predicted value of an observable by data and theory, respectively. Furthermore, σ_i is the error associated with the i th data point. Specifically, in our case, we have

$$\mathcal{L} = \sum_i A \exp\left[-\frac{1}{2} \left(\frac{D_i(z) - \sigma_8^0 \times \mathcal{T}_i(z)}{\sigma_i}\right)^2\right]. \quad (53)$$

We performed the likelihood analysis and found the maximum of σ_8^0 are 1.44 and 1.59, for MOG and mMOG, respectively. Since in MOG matter is entirely constituted by the baryonic fraction, we anticipated a larger value for σ_8^0 , compared to Λ CDM, to compensate for the smaller matter gravitational pull. A similar situation can be seen in [24].

In Fig. 4, we plot $f\sigma_8$ for MOG, mMOG and Λ CDM along with the data points. We have shown the long-term evolution of $f\sigma_8$ for all the models, to have a better insight about the models. We also fit a polynomial to the curves in MOG and mMOG. In the case of Λ CDM we picked the reported σ_8^0 in [19], while for MOG and mMOG we used the result of our likelihood analysis. As the plot clearly shows, the evolution of $f\sigma_8$ in MOG and Λ CDM is significantly different. Although χ^2/dof is smaller in MOG, one needs more data points to decide which model can fit the data more accurately.

¹It is necessary to mention that also $f\sigma_8$ is not completely model independent and in principle, one has to find it for the model under consideration. In the case of MOG, we can use the available data points, since MOG is designed to recover the same evolution for the background quantities as in Λ CDM

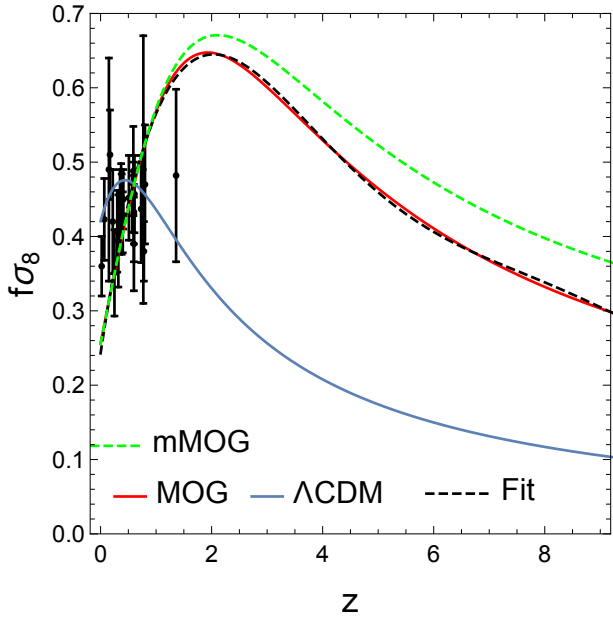


Figure 4: The long term evolution of $f\sigma_8^0$ for Λ CDM, mMOG with $c = 0.33 \times 8\pi$, MOG and the best fit with the 5th order polynomial $\sum_k A_k a^k$, where $A_5 = 8 \times 10^{-5}$, $A_4 = -0.00275$, $A_3 = 0.03544$, $A_2 = -0.20970$, $A_1 = 0.49936$ and $A_0 = 0.24289$.

We summarize all the results obtained from the likelihood analysis in Table 1. The main conclusion is that both MOG and mMOG predict larger values for σ_8^0 . Of course, to make a reliable decision on the viability of MOG as an alternative theory of dark matter, it is necessary to measure σ_8^0 from other relevant observations, like CMB and lensing [25]. We leave this point to future studies. In TeVeS, a relativistic version for Modified Newtonian Dynamics (MOND) [26], the vector field can play a role similar to cold dark matter [27] and increase the matter growth rate. However, our analysis shows that this is not the case in MOG, and the Proca vector field does not expedite the perturbation growth. Therefore, our conclusion can be considered a challenge to the viability of this theory.

It is necessary to mention another important issue. It has been shown in [28] that TeVeS leads to a huge enhancement of baryonic acoustic oscillations (BAO). Such behavior raises a serious challenge for the viability of TeVeS and is inconsistent with the observations. A similar enhancement in BAO can be seen in the context of MOG reported in [12]. The rapid oscillations in the power spectrum may be simply related to the fact that in absence of dark matter, baryons weigh more. However, it is necessary to revisit this important issue in MOG. The results presented in [12] are based on several approximations and analytic descriptions. On the other hand, the conventional and more reliable way to derive the angular power spectrum of CMB is to use the relevant numeric codes like CAMB [29] and explore the full set of parameters. Therefore, this code should be modified to include MOG effects. Of course, this is not easy and is well beyond the scope of our paper.

7. Discussion and Conclusion

In this paper, we investigated the cosmological perturbations in the context of a Scalar-Tensor-Vector theory of gravity known as MOG. As in the standard case, we started from the modified Friedmann equations and introduced the perturbed metric in the Newtonian gauge. We assumed that the matter content of the universe is a perfect fluid and, without imposing restrictive assumptions on the evolution of the fields, we found the first order perturbed field equations.

It is well known in the literature that any deviation from Λ CDM in matter dominated era may substantially influence the structure formation scenario. In order to consider this in detail, we evaluated the evolution of matter perturbations, δ , and the growth function, $f = \delta'/\delta$, in the context of MOG. Since the growth of gravitational seeds starts in the sub-horizon scale, we have considered the perturbed equations in the sub-horizon limit in the matter dominated epoch.

We also presented a similar description for mMOG, which is a different version of MOG compatible with the sound horizon observations. Our main result is that the growth of matter perturbations in both MOG and mMOG is slower than in Λ CDM. In fact, this is a surprising result, since in all the modified gravity theories aiming at replacing dark matter, the gravitational force should be strengthened in the weak field limit, in order to explain the flat galactic rotation curves, and other observations, without the pull of dark matter. However, we have shown that the reduced matter content of MOG overcompensates the extra gravitational force.

Table 1

σ_8^0 and χ^2/dof for Λ CDM, MOG and mMOG.

| Λ CDM | MOG | mMOG |
|-----------------------------|-----------------------------|-----------------------------|
| $\sigma_8^0 = 0.82$ [19] | $\sigma_8^0 = 1.44$ | $\sigma_8^0 = 1.59$ |
| $\chi^2/\text{dof} = 0.703$ | $\chi^2/\text{dof} = 0.651$ | $\chi^2/\text{dof} = 0.647$ |

We wrote down the full set of perturbation equations and determined the two modified gravity parameters, η and Y . We then compared MOG, mMOG and Λ CDM with the observed $f\sigma_8$, and found that MOG and mMOG require higher values for σ_8^0 . The RSD data do not yet rule out MOG but the high value of σ_8 seems problematic when compared to recent estimates due to lensing. Therefore we conclude that although MOG is not yet ruled out, a full analysis of CMB and lensing data will provide a strong challenge to MOG.

Acknowledgement

Sara Jamali thanks Henrik Nersisyan and Malihe Siavoshan for useful discussions. She also would like to thank the Institute for Theoretical Physics, University of Heidelberg for a very kind hospitality, during which some parts of this work have been done. Mahmood Roshan would like to thank Sohrab Rahvar for useful discussions.

References

- [1] J. W. Moffat. Scalar-tensor-vector gravity theory. *JCAP*, 0603:004, 2006.
- [2] Sara Jamali, Mahmood Roshan, and Luca Amendola. On the cosmology of scalar-tensor-vector gravity theory. *JCAP*, 1801(01):048, 2018.
- [3] J. W. Moffat and S. Rahvar. The MOG weak field approximation – II. Observational test of *Chandra* X-ray clusters. *Mon. Not. Roy. Astron. Soc.*, 441(4):3724–3732, 2014.
- [4] N. S. Israel and J. W. Moffat. The Train Wreck Cluster Abell 520 and the Bullet Cluster 1E0657-558 in a Generalized Theory of Gravitation. *Galaxies*, 6(2):41, 2018.
- [5] J. W. Moffat and S. Rahvar. The MOG weak field approximation and observational test of galaxy rotation curves. *Mon. Not. Roy. Astron. Soc.*, 436:1439–1451, 2013.
- [6] Pankaj Sheoran, Alfredo Herrera-Aguilar, and Ulises Nucamendi. Mass and spin of a Kerr black hole in modified gravity and a test of the Kerr black hole hypothesis. *Phys. Rev.*, D97(12):124049, 2018.
- [7] Federico G. Lopez Armengol and Gustavo E. Romero. Effects of Scalar-Tensor-Vector Gravity on relativistic jets. *Astrophys. Space Sci.*, 362(11):214, 2017.
- [8] M. A. Green, J. W. Moffat, and V. T. Toth. Modified gravity (MOG), the speed of gravitational radiation and the event GW170817/GRB170817A. *Phys. Lett.*, B780:300–302, 2018.
- [9] Luciano Manfredi, Jonas Mureika, and John Moffat. Quasinormal Modes of Modified Gravity (MOG) Black Holes. *Phys. Lett.*, B779:492–497, 2018.
- [10] Sara Jamali and Mahmood Roshan. The phase space analysis of modified gravity (MOG). *Eur. Phys. J.*, C76(9):490, 2016.
- [11] Fatimah Shojai, Samira Cheraghchi, and Hamed Bouzari Nezhad. On the gravitational instability in the Newtonian limit of MOG. *Phys. Lett.*, B770:43–49, 2017.
- [12] J. W. Moffat and V. T. Toth. Cosmological observations in a modified theory of gravity (MOG). *Galaxies*, 1:65–82, 2013.
- [13] J. W. Moffat and V. T. Toth. Fundamental parameter-free solutions in modified gravity. *Class. Quant. Grav.*, 26:085002, 2009.
- [14] J. W. Moffat. Structure Growth and the CMB in Modified Gravity (MOG). 2014. arXiv:1409.0853 [astro-ph.CO]
- [15] J. W. Moffat. Cosmological Evidence for Modified Gravity (MOG). 2015. arXiv:1510.07037 [astro-ph.CO].
- [16] Mahmood Roshan. Test particle motion in modified gravity theories. *Phys. Rev.*, D87(4):044005, 2013.
- [17] Ana Marta Pinho, Santiago Casas, and Luca Amendola. Model-independent reconstruction of the linear anisotropic stress η . *JCAP*, 1811(11):027, 2018.
- [18] Cinzia Di Porto and Luca Amendola. Observational constraints on the linear fluctuation growth rate. *Phys. Rev.*, D77:083508, 2008.
- [19] P. A. R. Ade et al. Planck 2015 results. XIII. Cosmological parameters. *Astron. Astrophys.*, 594:A13, 2016.
- [20] Surhud More, Hironao Miyatake, Rachel Mandelbaum, Masahiro Takada, David Spergel, Joel Brownstein, and Donald P. Schneider. The Weak Lensing Signal and the Clustering of BOSS Galaxies II: Astrophysical and Cosmological Constraints. *Astrophys. J.*, 806(1):2, 2015.
- [21] P. A. R. Ade et al. Planck 2015 results. XXIV. Cosmology from Sunyaev-Zeldovich cluster counts. *Astron. Astrophys.*, 594:A24, 2016.
- [22] Henrik Nersisyan, Adrian Fernandez Cid, and Luca Amendola. Structure formation in the Deser-Woodard nonlocal gravity model: a reappraisal. *JCAP*, 1704(04):046, 2017.
- [23] Imanol Albarran, Mariam Bouhmadi-López, and João Morais. Cosmological perturbations in an effective and genuinely phantom dark energy Universe. *Phys. Dark Univ.*, 16:94–108, 2017.
- [24] Niall MacCrann, Joe Zuntz, Sarah Bridle, Bhuvnesh Jain, and Matthew R. Becker. Cosmic Discordance: Are Planck CMB and CFHTLenS weak lensing measurements out of tune? *Mon. Not. Roy. Astron. Soc.*, 451(3):2877–2888, 2015.
- [25] H. Hildebrandt et al. KiDS-450: Cosmological parameter constraints from tomographic weak gravitational lensing. *Mon. Not. Roy. Astron. Soc.*, 465:1454, 2017.
- [26] Jacob D. Bekenstein. Relativistic gravitation theory for the MOND paradigm. *Phys. Rev.*, D70:083509, 2004. [Erratum: *Phys. Rev.* D71,069901(2005)].
- [27] Scott Dodelson and Michele Liguori. Can Cosmic Structure form without Dark Matter? *Phys. Rev. Lett.*, 97:231301, 2006.
- [28] Scott Dodelson, *Int. J. Mod. Phys. D*, 20:2749, 2011.
- [29] A. Lewis and S. Bridle, *Phys. Rev. D* 66:10351, 2002.